



Tetragonal high-pressure phase of InI predicted from first principles

Meiguang Zhang^{a,*}, Haiyan Yan^b, Gangtai Zhang^a, Qun Wei^c, Hui Wang^d

^a Department of Physics and Information Technology, Baoji University of Arts and Sciences, Baoji 721016, PR China

^b Shaanxi Key Laboratory for Phytochemistry, Department of Chemistry and Chemical Engineering, Baoji University of Arts and Sciences, Baoji 721013, PR China

^c School of Science, Xidian University, Xi'an 710071, PR China

^d National Laboratory of Superhard Materials, Jilin University, Changchun 130012, PR China

ARTICLE INFO

Article history:

Received 23 September 2011

Accepted 3 November 2011

Available online 9 November 2011

Keywords:

InI

Swarm optimization algorithm

High pressure transition

First principles

ABSTRACT

Ab initio particle swarm optimization algorithm for crystal structural prediction was employed to uncover the high-pressure crystal structure of indium iodide (InI). We have predicted one tetragonal high-pressure phase for InI with P4/nmm symmetry, which is energetically much superior to the previously proposed CsCl-type structure. The P4/nmm-InI possesses alternative stacking of double I and In layers. The arrangement of adjacent I and In layers of P4/nmm-InI is similar to that of the CsCl-type structure. The calculated electronic density of states supports a metallic character for this tetragonal phase that is similar to the high-pressure behavior of IIA–VIB families. Furthermore, the phase transition path from the ambient pressure TII–InI → P4/nmm-InI has been discussed.

© 2011 Elsevier B.V. All rights reserved.

1. Introduction

Indium halides have attracted much attention due to their unique physical and chemical properties in fundamental science and technological applications, such as high volatility at reasonably low temperatures, fast recombination rates fairly low dissociation energies, etc. [1–4]. One of indium halides, InI, is a promising semiconductor for radiation detector. The high atomic number of In and I, along with high density, give the InI detector a higher photon stopping power (attenuation coefficient) compared to Ge and comparable to that of CdTe. The resistivity of InI was reported to be very high, $\sim 10^{11} \Omega \text{ cm}$, at room temperature with a mobility lifetime product for electron $\sim 7 \times 10^{-5} \text{ cm}^2/\text{V}$. Another major advantage of InI is that both In and I are less toxic compared to other compound semiconductors used for fabrication of solid state detector such as CdTe (Cd), HgI₂ (Hg), and GaAs (As) [5–7].

Materials under high pressure exhibit rich transition behavior, which gives us broadened views into the essence of atomic binding in solids while greatly challenging our instinctive understanding. At ambient pressure, InI crystallizes in the base-center orthorhombic structure of TII-type (space group Cmcm) [8], which differs from that of the well investigated cubic thallium halides. However, the high-pressure behaviors of InI are rarely studied, and there is lack of confirmed reports on the existence of pressure-induced phase transitions. Recently, Becker and Beck [9,10] have investigated the high-pressure phase transitions of

TII-type compounds including InI by density functional theory (DFT) calculations. They proposed a however CsCl-type phase as the candidate structure at high pressure on account of its low Madelung energy, which becomes dominant in determining structures at small volumes. They determined this new high-pressure structure by energy calculations of different known possible structures. This procedure may miss some unexpected yet more stable structures. Accordingly, this question is open until the convincing proof is provided. The peculiarity and the absence of characterized high-pressure phase of InI prompted our endeavor to investigate its structural behavior at high pressure.

Here, we extensively explored the crystal structures of InI over a wide range of pressures (0–60 GPa) using a specifically developed particle swarm optimization (PSO) algorithm for crystal structure prediction [11,12]. This methodology has been successful in correctly predicting crystal structures for various systems including elements and compounds at high pressure [13–16], unbiased by any known information. We found one layer-like tetragonal P4/nmm structure, which is energetically more preferable than the previously proposed CsCl-type structure. The phase transition path from the TII-type → P4/nmm structure has also been discussed.

2. Computational details

Our PSO methodology on crystal structural prediction has been implemented in CALYPSO (Crystal structure AnaLYsis by Particle Swarm Optimization) code [12] at 0 GPa, 25 GPa, and 60 GPa with 1–4 formula units (f.u.) per simulation cell. The underlying

* Corresponding author. Tel./fax: +86 917 3364258.
E-mail address: zhmgbj@126.com (M. Zhang).

ab initio structural relaxations and electronic calculations were carried out using DFT within the Perdew–Burke–Ernzerhof exchange–correlation as implemented in the VASP code [17–19]. The all-electron projector augmented wave method [20] was adopted with $5s^25p^5$ and $4d^{10}5s^25p^1$ treated as valence electrons for I and In, respectively. The energy cutoff 400 eV and appropriate Monkhorst–Pack k meshes [21] were chosen to ensure that enthalpy calculations are well converged to better than 1 meV/atom. The phonon calculations were carried out using a supercell approach as implemented in the PHONOPY code [22].

3. Results and discussion

At 0 GPa, our simulations with the only input of chemical composition of In:I=1:1 predicted the most stable structure to be orthorhombic TII-type phase, in complete agreement with experiments. The TII–InI contains four f.u. per unit cell, and the I ions are fivefold coordinated and the In ions are sevenfold coordinated. Fig. 1a presents the crystal structure of the orthorhombic modification of TII projected on the bc -plane. Along the c -direction one can recognize zigzag chains of In–I sticks resembling the structure of trans-polyacetylene with In and I ions at the sites of C and H, respectively. Moreover, in order to provide some insight into the pressure behavior of TII–InI according to Ref. [9], the pressure dependences of the TII–InI lattice constants are plotted in Fig. 2, along with the experimental data and other theoretical results [9]. Strikingly, the calculated results are in agreement with these experimental data and theoretical values, indicating the reliability of our calculations.

The success in the prediction of TII-type structure gives us confidence to further explore the high-pressure phases of InI. For higher pressure at 20 GPa and 60 GPa, a new stable tetragonal P4/nmm phase having 2 f.u./cell (Fig. 1b) was discovered for InI. At 20 GPa, the optimized lattice parameters of P4/nmm–InI are $a=3.497$ Å and $c=7.771$ Å, with I and In atoms occupying $2c(0, 0, 0.1534)$ and $2c(0, 0, 0.6177)$ positions, respectively. This P4/nmm structure possesses alternative stacking of double I and In layers, and the coordination number of I and In ions increased up to 13. Each I ion is surrounded by five In ions and eight I ions (Fig. 1d), and each In ion is surrounded by five I ions and eight In ions (Fig. 1e), resulting in a similar polyhedron structure. We have performed the calculations on the phonon dispersion curves of P4/nmm–InI and CsCl–InI at 60 and 30 GPa, respectively. As shown in Fig. 3a, no imaginary phonon frequency was detected in the whole Brillouin zone for P4/nmm–InI, indicating its dynamical stability. For CsCl–InI shown in Fig. 3b, however, it is clearly seen that the phonon spectrum shows a large imaginary frequency at M point, signaling its structural instability.

To determine the phase transition pressure, we have plotted out the enthalpy curves of the P4/nmm–InI relative to the ambient-pressure TII–InI (Cmcm–InI) in Fig. 4a, and the CsCl–InI was also considered for comparison. It is confirmed that the TII–InI transforms to the predicted P4/nmm structure above 17 GPa, and thus the CsCl–InI can be ruled out as existing. Meanwhile, the calculated volumes as a function of pressure for TII–InI and P4/nmm–InI are also shown in Fig. 4b. The results suggest that TII–InI \rightarrow P4/nmm–InI phase transition is first-order with clear volume drops of 5.9%, which can be easily detected in further experiment. Furthermore, the thermodynamic stability of P4/nmm–InI at high pressure with respect to decomposition is quantified in terms of the formation enthalpy, $\Delta H_f = H_{\text{InI}} - H_{\text{I}} - H_{\text{In}}$. The ΔH_f is the formation enthalpy, the orthorhombic I (space group: Cmca) and tetragonal In (space group: I4/mmm) are chosen as the reference phases. The obtained results have demonstrated the structural stability of P4/nmm–InI against the decomposition into the mixture I and In up to 50 GPa.

Since Cmcm is a subgroup of P4/nmm, it is essential to investigate the relations between these two structures, which can help us to understand the mechanism of the Cmcm–InI \rightarrow P4/nmm–InI transition. In fact, as shown in Fig. 5(a) and (c), both Cmcm and P4/nmm are layer-like structures with the stacking order $KLKL\dots$ and $NN'MM'NN'\dots$. The transition path can be understood qualitatively as follows: for Cmcm structure, the I and In atoms in K layers are frozen, while the I and In atoms in L layers moved as a whole along b direction in ab planes during

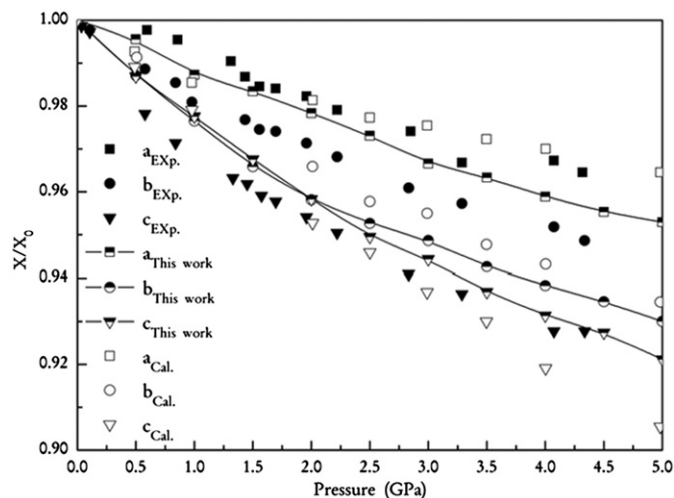


Fig. 2. Pressure dependences of lattice constants for TII–InI, together with the experimental data and other theoretical values.

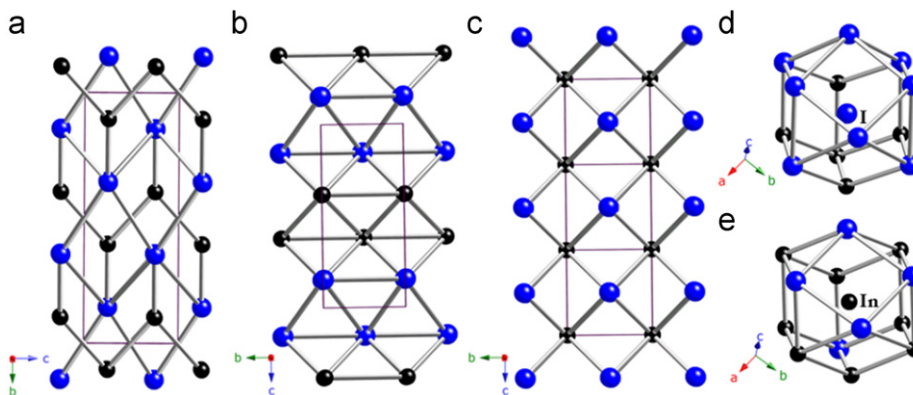


Fig. 1. Crystal structures of InI for TII-type (a), P4/nmm (b), and CsCl-type (c). The large and small spheres represent I and In atoms, respectively.

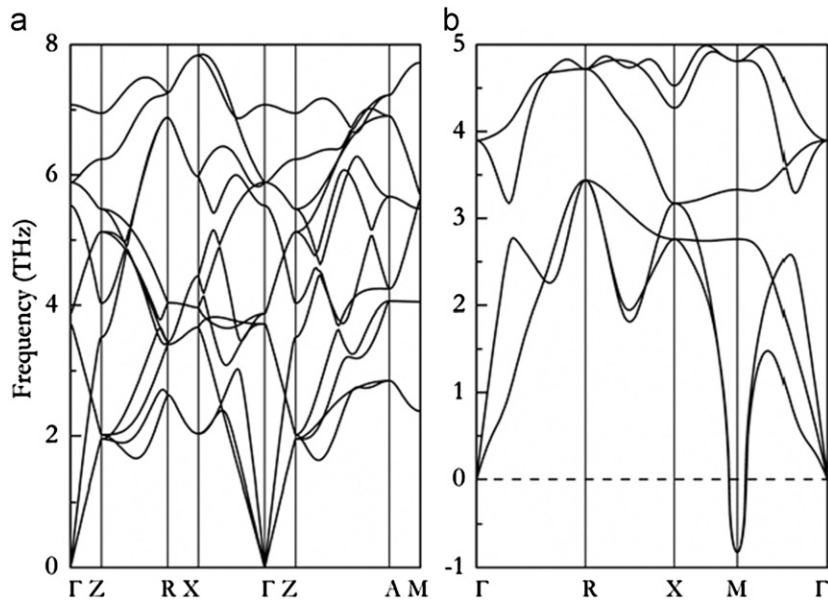


Fig. 3. Phonon dispersion curves of P4/nmm-InI at 30 GPa (a) and those of CsCl-InI at 60 GPa (b).

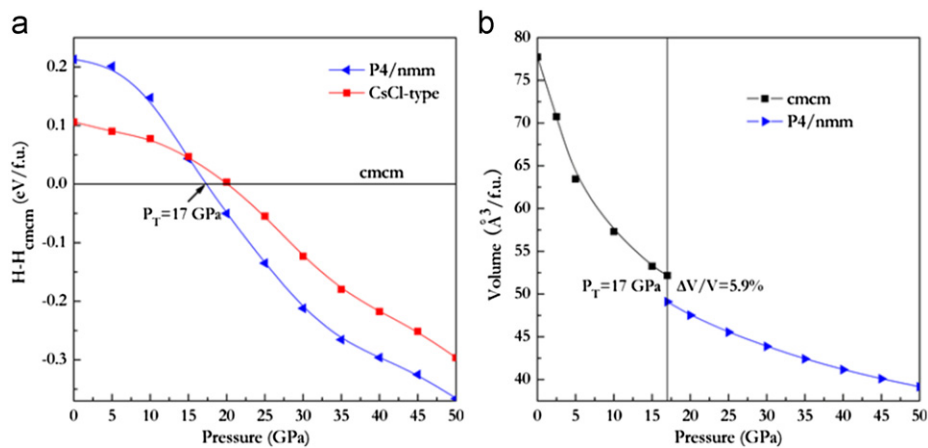


Fig. 4. The calculated enthalpies per f.u. of the P4/nmm-InI relative to Cmcm-InI as a function of pressure (a) and the calculated volumes as a function of pressure for Cmcm-InI and P4/nmm-InI (b).

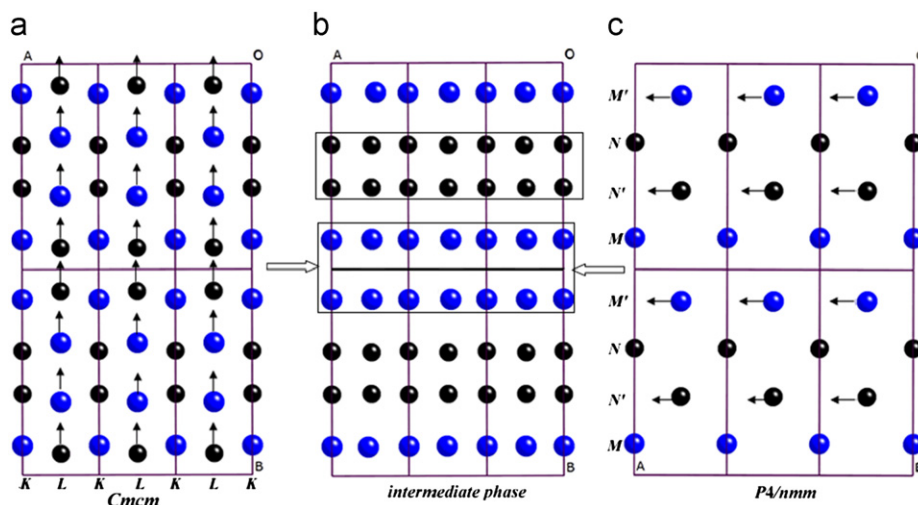


Fig. 5. The Cmcm-InI viewed along the c-axis (a), the intermediate phase viewed along the c-axis, showing the arrangement of double I and In layers (b), and the P4/nmm-InI viewed along the b-axis (c). Arrows in (a) indicate the displacements of I and In atoms in L layers related to the Cmcm-InI \rightarrow intermediate phase, and arrows in (c) indicate the displacements of I and In atoms in M' and N' layers related to the P4/nmm-InI \rightarrow intermediate phase.

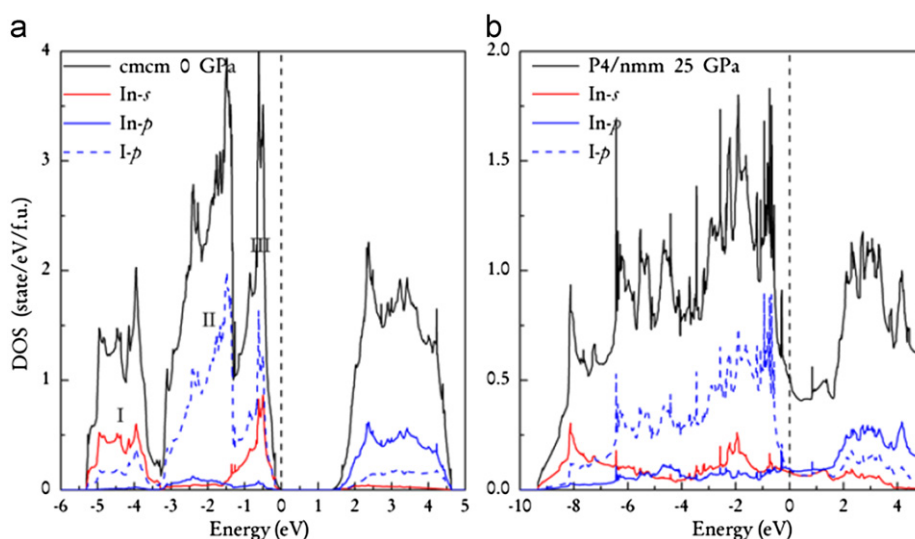


Fig. 6. Total and partial densities of states of TlI-InI at 0 GPa (a) and P4/nmm-InI at 25 GPa (b). The vertical dashed line denotes the Fermi level at zero.

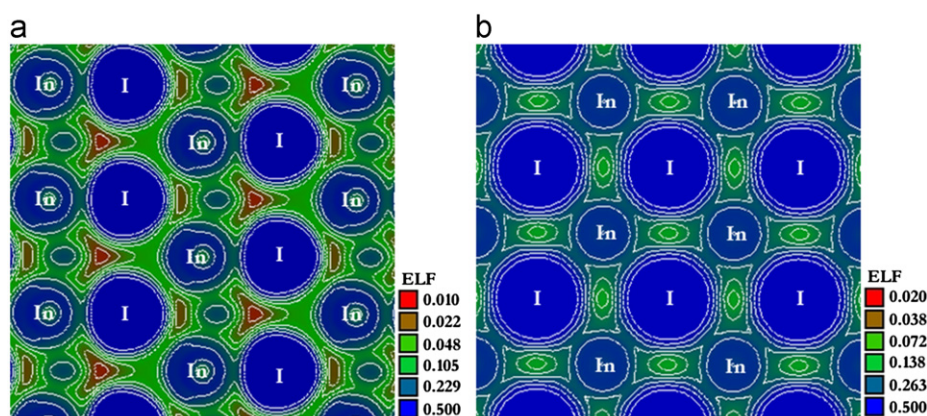


Fig. 7. Contours of ELF of TlI-InI on the (0 0 1) plane at 0 GPa (a) and those of P4/nmm-InI on the (0 0 1) plane at 25 GPa (b).

compression (by the arrows in Fig. 5a). Such atomic displacements result in an alternative stacking of double I and In layers along b axis, named intermediate phase, as illustrated in Fig. 5b. Obviously, for the P4/nmm structure, the displacement of I atoms in M' layers and In atoms in N' layers along a direction (by the arrows in Fig. 5c) can also form the same arrangements of I and In atoms to those of the intermediate phase. Accordingly, the Cmcm-InI \rightarrow P4/nmm-InI transition path can be connected by this intermediate phase.

Atomic displacements are always accompanied by a striking change of properties, especially electronic properties. Therefore, the total and site projected electronic densities of states (DOS) of TlI-InI and P4/nmm-InI were calculated at ambient pressure and 25 GPa. As expected (Fig. 6a), the TlI-InI is a semiconductor characterized by an energy gap of ~ 1.38 eV, which agrees well with previous reports [8–9,23]. From inspection of its partial DOS curves, we could see three groups of states, depicted as I, II, and III in the valence band region. Part II is mainly dominated by I-5p states mixed with slight contributions of In-5p states. Part I and part III are characterized by a mixture of In-5s and I-5p states. The admixture of In⁺ 5p states can be seen in peaks of II and III of DOS curve of TlI-InI. Conclusively, the DOS curves of TlI-InI are in agreement with a predominantly ionic description and weak covalent interactions. Compared to the TlI-InI, P4/nmm-InI exhibits clear metallic behavior by evidence of the finite electronic DOS at the Fermi level (Fig. 6b). The increased overlap of different peaks leads to a large interaction between neighbors, and thus to

a larger bandwidth and a smaller DOS. In addition, the ionic nature of the two structures is demonstrated by the corresponding Electronic Localization Function (ELF) [24–25] analysis, as depicted in Fig. 7. One can note I–In ionic bonds with nearly identical I–In ionic “point attractors” at ELF=0.229 for TlI-InI on the (0 0 1) plane and ELF=0.263 for P4/nmm-InI on the (0 0 1) plane.

4. Conclusions

In summary, we have found that the experimental TlI-InI transforms to a tetragonal metallic P4/nmm structure at 17 GPa, using particle swarm optimization algorithm for crystal structural prediction. This finding rules out the earlier belief of the TlI-InI \rightarrow CsCl-InI high-pressure transition. The stability of P4/nmm-InI is justified by the enthalpy calculations, and its dynamical stability has been confirmed by the phonon calculations. The phase transition path of TlI-InI \rightarrow P4/nmm-InI has been identified as the displacement of I and In layers under compression.

Acknowledgment

This work is supported by Baoji University of Arts and Sciences Key Research (Grant No. ZK1032, ZK0918, ZK10122), the Phytochemistry Key Laboratory of Shaanxi Province

(Grant No. 11JS008), and the Fundamental Research Funds for the Central Universities.

References

- [1] J. Maya, Appl. Phys. Lett. 32 (1978) 484.
- [2] H. Hemmati, G.J. Colline, Appl. Phys. Lett. 34 (1979) 844.
- [3] S.K. Mishra, Raj K.S. Yadav, V.B. Singh, S.B. Rai, J. Phys. Chem. Ref. Data 33 (2004) 453.
- [4] M.H. Du, D.J. Singh, Phys. Rev. B 82 (2010) 045203.
- [5] K.S. Saha, P. Bennet, L.P. Moy, M.M. Misra, W.W. Moses, Nucl. Instrum. Methods Phys. Res. A 380 (1996) 215.
- [6] P. Bhattacharya, M. Groza, Y. Cui, D. Caudel, T. Wrenn, A. Nwankwo, A. Burger, G. Slack, A.G. Ostrogorsk, J. Cryst. Growth 312 (2010) 1228.
- [7] T. Oondera, K. Hitomi, T. Shoji, IEEE Trans. Nucl. Sci. 50 (2006) 3055.
- [8] R.E. Jones, D.H. Templeton, Acta Crystallogr. 8 (1995) 847.
- [9] D. Becker, H.P. Beck, Z. Anorg. Allg. Chem. 630 (2004) 40.
- [10] D. Becker, H.P. Beck, Z. Anorg. Allg. Chem. 219 (2004) 348.
- [11] Y. Wang, J. Lv, L. Zhu, Y. Ma, Phys. Rev. B 82 (2010) 094116.
- [12] Y. Ma, Y. Wang, J. Lv, L. Zhu, <<http://nlshmlab.jlu.edu.cn/~calypso.html>>.
- [13] J. Lv, Y. Wang, L. Zhu, Y. Ma, Phys. Rev. Lett. 106 (2011) 015503.
- [14] L. Zhu, H. Wang, Y. Wang, J. Lv, Y. Ma, Q. Cui, Y. Ma, G. Zou, Phys. Rev. Lett. 106 (2011) 145501.
- [15] P. Li, G. Gao, Y. Wang, Y. Ma, J. Phys. Chem. C 114 (2010) 21745.
- [16] H.Y. Liu, Q. Li, L. Zhu, Y.M. Ma, Solid State Commun. 51 (2011) 576.
- [17] W. Kohn, L.J. Sham, Phys. Rev. 140 (1965) A1133.
- [18] J.P. Perdew, K. Burke, M. Ernzerhof, Phys. Rev. Lett. 77 (1996) 3865.
- [19] G. Kresse, D. Joubert, Phys. Rev. B 59 (1999) 1758.
- [20] P.E. Blöchl, Phys. Rev. B 50 (1994) 17953.
- [21] J.D. Pack, H.J. Monkhorst, Phys. Rev. B 16 (1977) 1748.
- [22] A. Togo, F. Oba, I. Tanaka, Phys. Rev. B 78 (2008) 134106.
- [23] M.I. Kolinko, J. Phys.: Condens. Matter 6 (1994) 183.
- [24] A.D. Becke, K.E. Edgecombe, J. Chem. Phys. 92 (1990) 5397.
- [25] A. Savin, B. Silvi, Nature 371 (1994) 683.